Anal. Bioanal. Electrochem., Vol. 9, No. 6, 2017, 673-688

Analytical & Bioanalytical Electrochemistry

www.abechem.com

Full Paper

Nitrate Effect on Degradation Processes of α,(α+β)-brasses in Moroccan Azrou Soil Medium

Mouhsine Galai,[1,*] Hanane Benqlilou,[2] Mohamed Ebn Touhami,[1] Tounsi Belhaj,[2] Khalifa Berrami,[2] Ilyas Mansouri,[2] Hakima Nassali[1] and Bennaceur Ouaki[3]

[1]*Laboratory of Materials Engineering and Environment: Modelling and Application, Faculty of Science, University IbnTofail BP. 133-14000, Kenitra, Morocco*
[2]*International Institute for Water and Sanitation (IEA), National office of Electricity and the Potable Water, Morocco*
[3]*Ecole Nationale Superieure des Mines de Rabat, Morocco*

*Corresponding Author, Tel.: +212677235695
E-Mail: galaimouhsine@gmail.com

Received: 15 January 2017 / Accepted: 7 August 2017 / Published online: 30 September 2017

Abstract- Usually, nitrates are found naturally in low concentrations in water, but they can also have an artificial origin due to their use as crop fertilizer (mineral and organic fertilizers, animal manure). Excess not absorbed by plants are leached by rain and remains in the soil. In this paper we are going to study the effect of nitrates (NO_3^-) existence in soil on metal degradation of two series of brass (α and α+β) used as a support fittings which are suitable for connecting domestic service lines. This work aims at specifying the best alloys which are recommended to be used in Moroccan Azrou soil medium. This research paper was applied by using electrochemical impedance spectroscopy (EIS) methods and polarization curves. It was found that EC6 is the most resistant alloy between all brasses in this soil which containing 2 g/L of NO_3^-. Moreover, we have studied the role and effects of various additional elements which exist in different brasses and they are responsible for increasing the corrosion resistance.

Keywords- Corrosion, Brass, Soil, Nitrate, Polarization curves, EIS

1. INTRODUCTION

Brass alloys represent an important category of materials that meet the requirements of many industrial applications. Like most metallic materials, brass alloys suffer from corrosion.

Selective leaching of the active component of the alloy represents the major corrosion problem. Dezincification of brass alloys leads to the loss of valuable physical and mechanical properties [1] and to total failure of the material. Dealloying processes, which occur in nonferrous alloys, are dependent upon their electrochemical properties. Dezincification or the preferential dissolution of zinc from brass is known for decades. The two general mechanisms postulated to explain this phenomenon are selective dissolution of zinc [2,3] and simultaneous dissolution of both copper and zinc with the subsequent re-deposition of copper [4,5]. The preferential dissolution of zinc leads to a porous and friable layer of corrosion products of copper at the surface. The addition of small amounts of tin [6,7] and elements like arsenic, antimony and phosphorous [8,9,10] improves the dezincification resistance of brasses in various aggressive environments.

Otherwise; Brass, because of its strength, are frequently used in underground installations. However, soil composition, particularly the presence of fertilizers in agriculture, acid rain and marine intrusion, greatly affects the corrosion resistance of buried metallic materials [11].

The present work investigates the effect of nitrate ion content on the behavior of two series of brasses used in the drinking water distribution network in a clay soil of the region from Azrou of Morocco. Moreover corrosion tests were performed in $NaNO_3$ solution only [12] but not in modified soil containing NO_3^- ions, although in literature the solutions that are most often used are ammonia [13] sulfuric acid [14,15] and nitrite solutions [16]

The figure 1 show examples of the degradations observed on brass devices used as a support fittings which are suitable for connecting domestic service lines.

Fig. 1. Example of deterioration of support fittings which are suitable for connecting domestic service lines buried in the Azrou soil

2. MATERIALS AND METHODS

2.1. Materials

2.1.1. Soil sample preparation

A fraction of the soil collected in a suburban area of Azrou, in morocco, was dried at 105°C for 24 h and then left in the desiccator. Soil sampling and analysis is performed following the procedures described elsewhere [17].

Table 1 gives the concentrations of the elements and the texture that have been analyzed in the original soil sample, the studied soil materials comprise of 41.2% silt, 35.6% clay and 23.2% sand giving rise to classify such soil as clay soil.

Table 1. Main features of the Azrou soil as received from the field and properties of the soil

Eléments (mg/l)	Ca^{2+}	Mg^{2+}	Cl^-	SO_4^{2-}	Na^+	K^+	*TAC*	*TH*
	17.6	3.9	7.1	5	4.14	4.3	1	1.2
Chemical	*pH*	*CE (mS/cm)*		NH_4^+ *(méq/l)*		$N0_3^-$ *(méq/l)*		*TH (%)*
properties	7,21	0,138		0,11		0,10		19
Texture (%)	$CaCO_3$	*A*	*L*	*S*	*LF*	*LG*	*SF*	*SG*
	39,5	35,6	41,2	23,2	15,3	25,9	10,6	12,6

The original soil sample was modified by adding calculated amounts of $NaNO_3$. The procedure used in the preparation of the modified soil samples and its identification is given in Table 2. The volume of demineralized water or modifier solution added to the weighted dried soil was calculated in order to give a relative humidity (RH) of 14%. The sample sol_{mod} was prepared in a way that the added solution containing 2 g/l of $NaNO_3$.

Table 2. Composition of various soil samples

Soil sample	***Composition of solution (× : with / - : without)***		***Moisture content %***
	Demineralized water	***$NaNO_3$(2g/L)***	
Original soil	×	-	14
Modified ($soil_{mod}$)	×	×	14

In addition, the electrochemical cell which was specifically designed for this study is represented in (Fig. 2) by respecting the literature **[**18**]**.

Fig. 2. Electrochemical system designed for the study of brasses coupons in soil

Each soil sample was compacted manually in the electrochemical cell by applying a Proctor Compactor that consists of 3 kg soil which is dropped from a height of 300 mm. The atmosphere inside the cell was constantly renewed via a flow of reconstituted air (80% of N_2 and 20 % of O_2) which circulated on the soil surface in the upper part of the cell.

2.1.2. Composition of various brasses

Various types of brass alloys under investigation were classified in two types α-brass and *α+β* brass. The chemical composition of these alloys is recorded in Table 3. Chemical composition analysis is performed by optical emission spectrometer (OES).

Table 3. Chemical compositions of α-brasses and α+β brasses with addition element

Brass	***Composition, wt. %***												
Samples	***% α***	***Cu***	***Zn***	***Pb***	***Sn***	***Fe***	***Al***	***Ni***	***As***	***Mn***	***P***	***Si***	***Sb***
EC1	60.09	57.5	36.85	2.96	1.135	0.58	0.2435	0.34	0.011	0.068	0.00235	0.0595	0.053
EC2	61.51	56.1	36.83	4.16	1.41	0.86	0.043	0.315	0.018	0.014	0.0013	0.023	0.056
EC3	87.1	59	37.06	2.8	0.28	0.25	0.056	0.10	0.12	0.022	<0.0001	0.076	0.04
EC4	52.73	56.7	38.1	2.7	0.85	0.46	0.417	0.36	0.02	0.033	0.002	0.057	0.053
EC5	92.86	62.6	34.91	1.96	0.16	0.11	<0.001	0.05	0.089	<0.0005	<0.0001	<0.0005	0.024
EC6	62	58.8	37.14	1.99	0.89	0.515	0.096	0.20	0.018	0.0715	0.004	0.040	0.036
EC7	91.27	70	21.95	1.27	0.57	1.71	3.675	0.45	0.010	0.1365	0.00165	0.0345	0.03

The working electrode consists of a piece of brass were wrapped by copper conductor wires tightly except for the top and bottom faces, and then covered by epoxy resin entirely except for an area of 0.78 cm^2 exposed to the soil, the coupons of brass abraded with emery

paper (up to 1200 grit) finally, washed by the deionized water, degreased by alcohol and dried naturally respectively.

2.2. Electrochemical methods

2.2.1. Electrochemical impedance spectroscopy

Electrochemical impedance spectroscopy (EIS) measurements were performed using a transfer function analyzer (VoltaLab PGZ100) frequency response analyzer in a frequency range of 100 kHz to 10 mHz with 10 points per decade. The EIS diagrams were done in the Nyquist representation. The results were then analyzed in respecting of an equivalent electrical circuit by Bouckamp program [19].

2.2.2. Polarization tests

The counter electrode was a stainless steel plate of large surface area and reference electrodes were copper–copper sulphate electrodes $Cu/CuSO_4$ (+0.316 V/SHE at 25 °C) which were commonly used in the field. In the following parts of this article, all potentials are presented relate with this reference electrode.

In addition the working electrode was immersed in the soil during 21 days until a steady state open circuit potential *(E_{ocp})* was obtained. The steady-state polarization curves were recorded potentiodynamically using a Volta Lab PGZ 100 and controlled by a personal computer. The cathodic polarization curve was recorded by polarization from *(E_{ocp})* to negative direction(-1500 mV/Cu/$CuCuSO_4$) under potentiodynamic conditions corresponding to 1 mVs^{-1} (scan rate) After this scan, the anodic polarization curve was recorded by polarization from *(E_{ocp})* to positive direction (1200 mV/ Cu/$CuCuSO_4$) under the same conditions as said before. The corrosion kinetic parameters were evaluated again by means of nonlinear least square method and by applying Eq. (1) using Origin software. Nonetheless, for this calculation, the potential interval that applied was limited to±0.100 V beside E_{corr}, and a significant systematic divergence was sometimes noticed for both cathodic and anodic branches.

$$i = i_a + i_b = i_{corr} \times \{\exp[b_a \times (E - E_{corr})] - exp[b_c \times (E - E_{corr})]\} \quad (1)$$

Where i_{corr} (corrosion current density (A cm^{-2})) and b_a and b_c (the Tafel constants of anodic and cathodic reactions (V^{-1}) respectively), these constants are attached to the Tafel slopes β (V/dec) in usual logarithmic scale which is given by the following equation:

$$\beta = \frac{\ln(10)}{b} = \frac{2.303}{b} \quad (2)$$

3. RESULTS AND DISCUSSION

3.1. Potentiodynamic polarization curves

Figure 3 shows the polarization curves of the two series of brass studied (α -brass and (α+β) brass) in Azrou soil modified by the addition of 2 g/L of $NaNO_3$ (sol_{mod}) after 21 days of immersion in this soil. To take into account the low conductivity of the soil studied in this work, the polarization curves are corrected by the ohmic drop (Rs: resistance of the soil is quite large in the order of 100 Ω.cm2). Their corresponding parameters like corrosion current density (i_{corr}), anodic (β_a) and cathodic (β_c) Tafel slopes and corrosion potential (E_{corr}) of all studied systems were fitting by Stern–Geary equation and registered in Table 4.

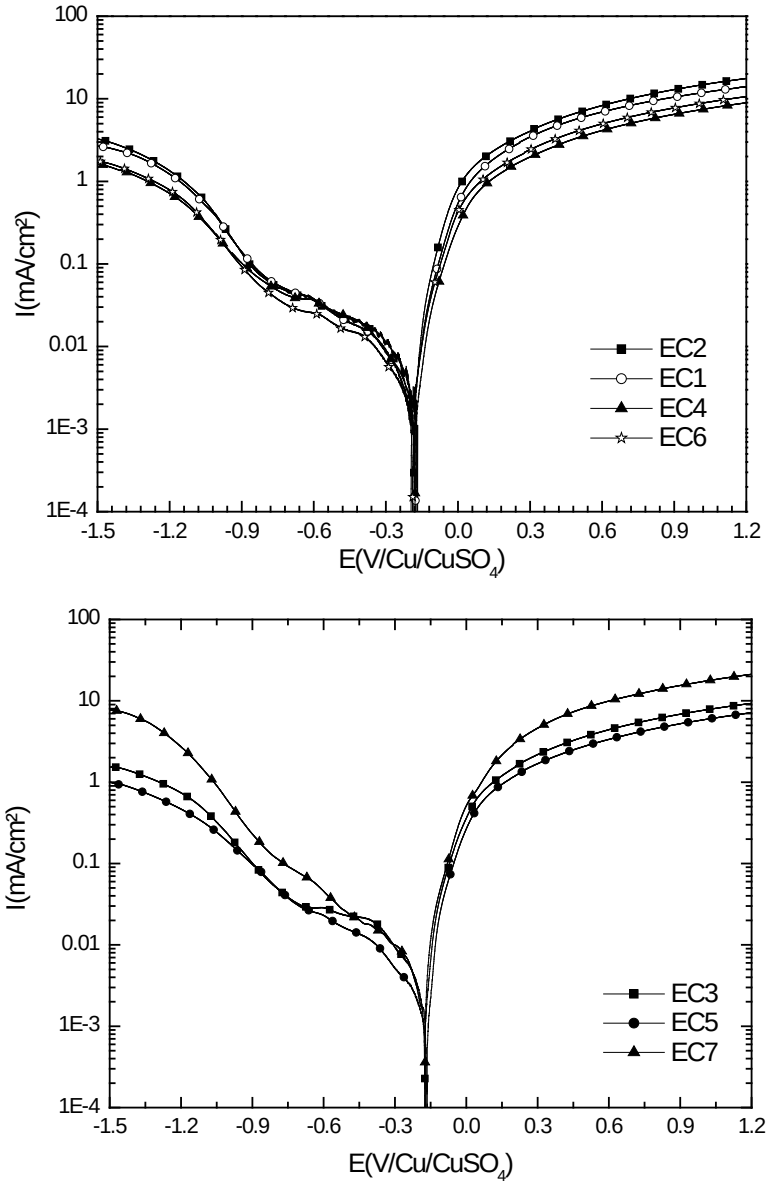

Fig. 3. Polarization curves for α+β brasses (a) and α-brasses (b) electrode in soil sample (sol_{mod}) after 21days of immersion at 14% of moisture content

For example, Fig. 4 shows a comparison of experimental and fitting data using a non-linear fitting with Stern–Geary equation for different brass electrodes in $soil_{mod}$ after 21 days of immersion.

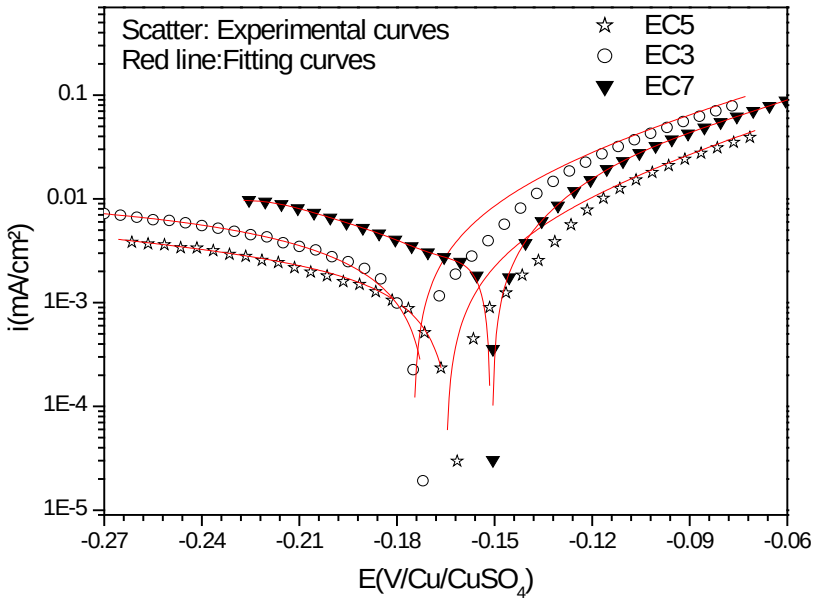

Fig. 4. Comparison of experimental (scatter) and fitting (red line) data using a non-linear fitting with Stern–Geary equation for different brass electrodes in soil sample $soil_{mod}$ after 21days of immersion

The cathodic branch shown in Figure 3(a) and 3 (b) reveals the existence of the two domains: the first range between the corrosion potential and -0.4 V/Cu /$CuSO_4$ and the current plateau down to -0.8 V/Cu/$CuSO_4$. This limit current density corresponds to the current of the dissolved oxygen reduction. The same behavior has already been observed in the works of Deslouis and Col [20].

These authors have clearly established that the layer of corrosion products, composed essentially of Cu_2O, does not affect this cathodic process: the electrode is always accessible to the reduction of oxygen or water. Other authors say that the cathodic branch is complex and involves other reduction reactions than those of water and oxygen with the reduction of NO_3^- and then NO_2 ions (Formation of NO_2^-) [21].

The anodic branch shown in figure 2 (a) and 2 (b) represents two regions:

- In region I, we can notice that the current density increases rapidly from E_{corr} to E=0.25 V/Cu/$CuSO_4$. This increase can be attributed to the dissolution of Zn which is rapidly activated, such as the oxidation of Cu.
- In region II, the current density remains substantially constant (passive region).This plateau is attributed to the formation of protective oxide film on surfaces of brasses [22]

Table 4. Polarization curves parameters for different brasses after 21 days of immersion in soil sample (sol_{mod}) after 21days of immersion at 14% of moisture content

Brass grad		**E_{corr}** ***(mV/ Cu/CuSo4)***	**i_{corr}** **(µA/cm²)**	**β_c** ***(mV dec^{-1})***	**β_a** ***(mV dec^{-1})***
(α+β) Brass	EC1	-176	6,01	-132	79
	EC2	-166	15.7	-140	77
	EC4	-176	8.2	-215	81
	EC6	-186	5,25	-214	75
α-Brass	EC3	-173	8.5	-233	85
	EC5	-162	7.1	-131	88
	EC7	-150	11	-89	90

The NO_3^- ions are very aggressive for brass, so the dezincification process has been accelerated. This effect is pronounced in the case of the brass with a single phase α.

More precisely, Fernandez in 2011[23] hypothesized the aggressiveness of these ions based on a "local acidification mechanism" proposed by Galvele in 1976 [24] to explain the corrosion observed after the rupture of Level of passivity. This mechanism is based on two hypotheses:

-The aggressive ions are anions of strong acids NO_3^- in this case. These do not form insoluble products when they are in contact with the metal because $Cu(NO_3)_2$ and $Zn(NO_3)_2$ are very soluble in water.

-The alloy reacts with OH^- ions, resulting a drop in pH at the surface of the anode according to Equation 3 and / or Equation 4.

$$Zn^{2+} + 2HO^- \rightarrow Zn(OH)_2 \quad (3)$$

$$Cu^{2+} + 2HO^- \rightarrow Cu(OH)_2 \quad (4)$$

This local acidification at the surface of the material promotes the corrosion by causing the migration of aggressive anions to the surface in order to preserve the electro-neutrality of the highly impoverished OH^- electrolyte. The anions then make it possible not only to continue the local acidification (Equation 2 & Equation 2), due to the displacement of the equilibrium of the charges but also to continue the dissolution, due to the consumption of the Zn^{2+} and Cu^{2+} ions present in solution. NO_3^- ions could have a catalytic effect on the production of the hydroxides.

This local acidification mechanism is consistent with the weak influence of NO_3^- ion concentration, which suggests an unlikely involvement of nitrate complexing reactions, in parallel with the important role of pH on the passivation mechanisms. It is true that the initial

basic medium may leave perplexing on a sufficiently strong acidification on the surface of the sample. However, even a small decrease in pH could destabilize the oxides that create passivity or pseudo-passivity [21].

The nitrate solutions still allow the formation of the complexes such as $CuNO_3^+$ or $ZnNO_3^+$, but these complexes do not substantially widen the dissolution domains of copper and zinc observed for ammoniacal solutions as shown in Figure 5 for copper.

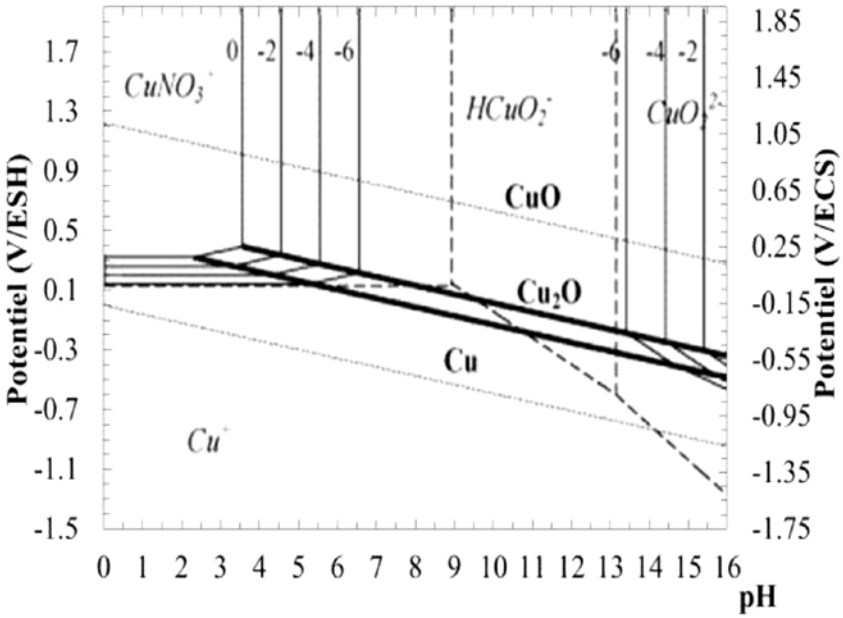

Fig. 5. Diagram Potential-pH of the Cu-NO_3^--H_2O system

It noticed from table 4 that the corrosion current density of EC6 is lower than the other duplex alloys two times and we can follow this classification:

$EC_6>EC_1>EC_4>EC_2$

The last following classification of these $\alpha+\beta$ brasses is can be due to effects of synergy among the various elements of addition. Nevertheless, it is difficult to establish the individual effect of elements on corrosion resistance and the rates of dezincification because this can have effects on synergy for certain combinations of further elements. Moreover, the literature demonstrates that the formation of a film which is formed on the alloy surface has an effect on dezincification rate [25].

Other investigators [26] have investigated the influence of Nickel, the Nickel alone had no inhibitive role. A synergistic effect of nickel and tin was found when certain concentrations were added at it. These were tin concentrations as high possible as up to 0.7% and 0.5% Ni, the depth of corrosion was reduced [7]. The brass EC6 is the most resistant compared with the alma EC2 and other brass because it had a synergic effect between Sn and Ni according to **[**7**]** and it had a small percentage of Fe relative which is responsible of

accelerating dezincification brass [27]. Concerning the α-brasses, we can follow this classification:

EC5>EC3>EC7

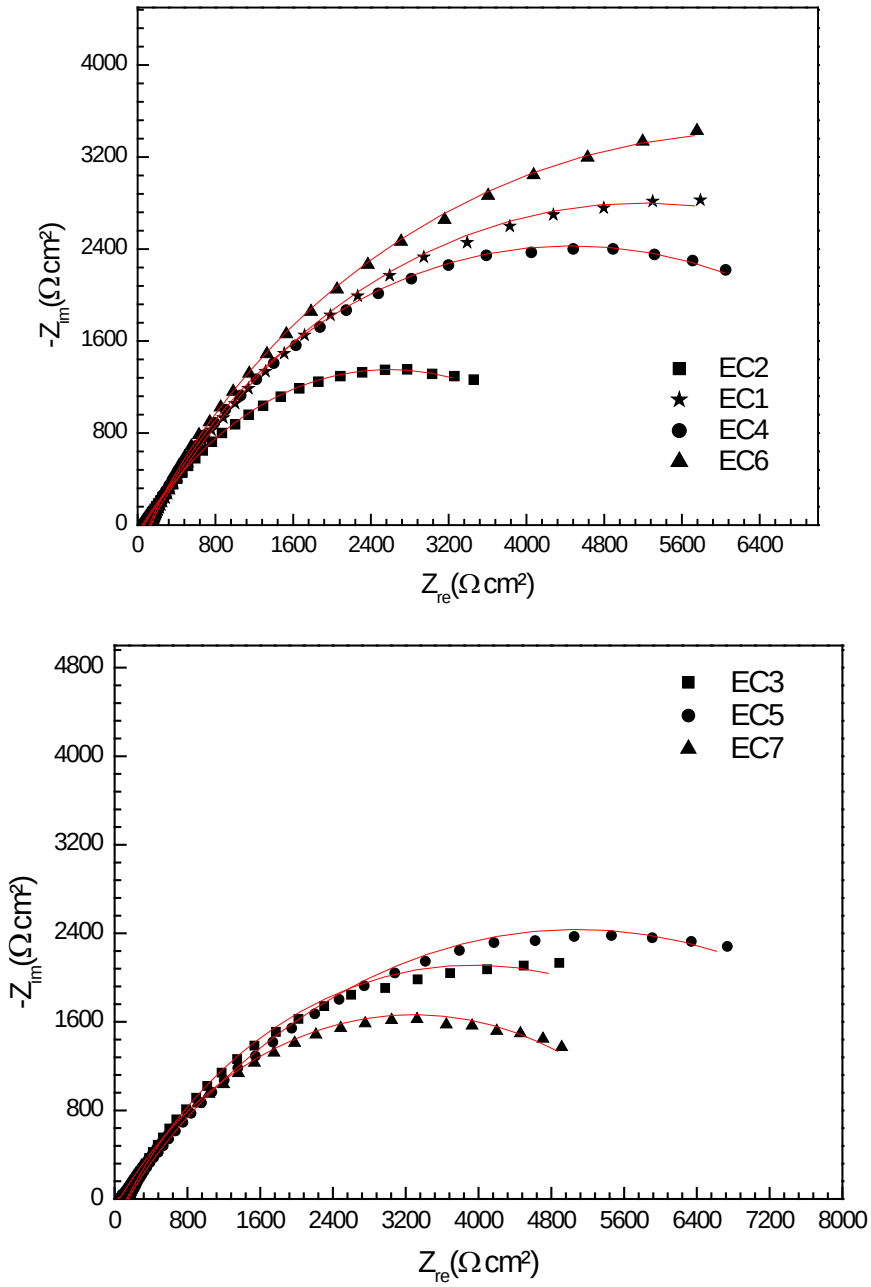

Fig. 6. Nyquist plots recorded for $\alpha+\beta$ brasses (a) and α-brasses (b) electrode in soil sample (sol_{mod}) after 21days of immersion

We can explain this classification as:

- The presence of arsenic in the chemical composition of brass decreases the corrosion rate. Many authors [28,29] found that a small quantity of arsenic inhibited the preferential

dissolution of zinc from the all alpha brasses. In addition Hollomon and Wulff [30] said that the minimum corrosion rate is obtained with an arsenic addition of 0.084%, in comparing with our study is the case of the alloy EC5.

- EC5 contains a lower percentage of Fe and Mn than the alloy EC3 and EC7 indeed the both elements are accelerators of brass dezincification [31].

3.2. Electrochemical Impedance Spectroscopy (EIS)

The tests were carried out by the electrochemical impedance spectroscopy to assess the corrosion resistance in comparison with the seven alloys. The impedance diagrams were obtained in the Nyquist representation at E_{ocp} between 100 KHz and 10 mHz in soil sample sol_{mod}. Figure 6 shows the impedance diagrams recorded under open circuit conditions after 21 days, relative to two series of brass (α -brass and (α+β) brass) .

It is important to make sure that such diagrams obtained experimentally are really significant before devising an electrochemical model. In this context, the Kramers-Kronig transforms offers a useful tool to validate the measured results before undertaking any further investigation. Some authors claimed that a certain impedance feature cannot be verified through the Kramers-Kronig transforms even though the results are reproducible and verify the linearity [32,33,34] .

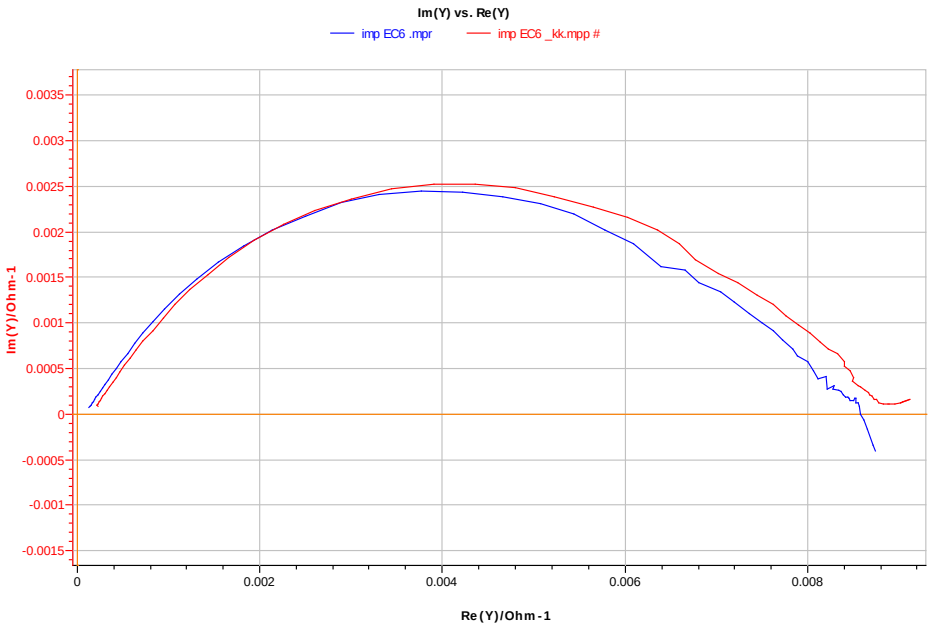

Fig. 7. Kramers-Kronig transformation for brass EC6 electrode in soil sample (solmod) after 21days of immersion; red line is experimental curve, blue line is Kramers-Kronig transformation

If the impedance is measured under potential regulation, the validity test should be performed with admittance. Conversely, if transfer functions are obtained under current regulation, the Kramers-Kronig transform should be applied to the electrode impedance. for example the figure 7 shows a comparison of experimental and Kramers-Kronig transformation for one brass named EC6 Immersed in $soil_{mod}$ after 21 days of immersion.

The result of the transforms agrees quite well with the initial data as can be seen by the comparison of Figure 7. So we can say that the Kramers-Kronig transformation evaluated our experiments tests. The impedance data of the EC6 brass recorded after 21 days of electrode immersion in soilmod are presented as Bode plots in Figure 8.

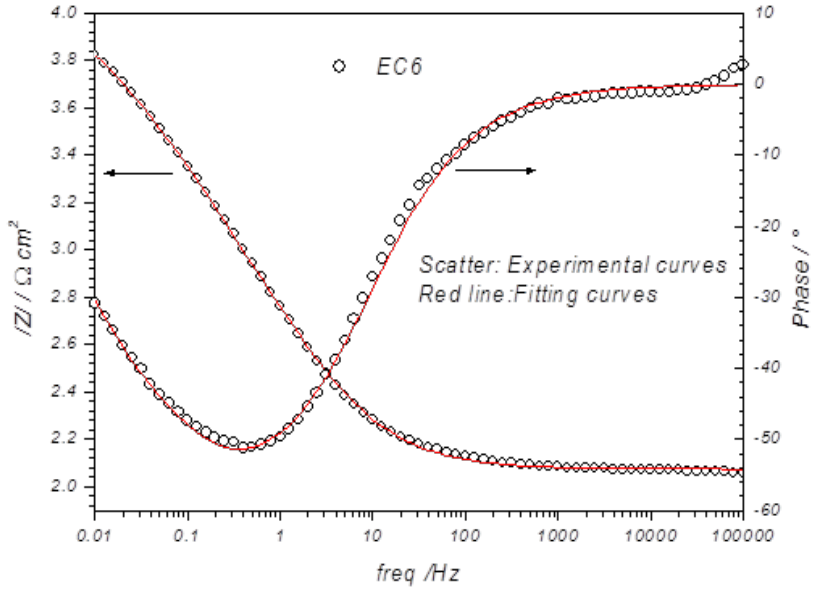

Fig. 8. Bode plots of EC6 alloys after 21 days of immersion in soil sample (sol_{mod})

The Bode plots show two phase maxima at intermediate and low frequencies. The presence of a second phase maximum, at low frequencies, and The absence of the impedance plateau indicate the presence of a diffusion process **[**35].

The response of the system to the imposed frequency variations can be represented by an equivalent electrical circuit which involves different contributions corresponding to the various frequency ranges. Thus, the circuit envisaged takes account of the low frequencies, the resistance of the electrolyte R_s and the faradic impedance which encompasses the charge transfer resistance R_t and the capacity of the double layer C_{d1}.

At the high frequencies, the capacitive loop observed is attributed to the dissolution of the metal matrix and to the formation of the passive film. Ideally represented by a circuit R//C, it is necessary to take into account here a deviation which is characterized by a circle not centered on the abscis axis. This deviation is usually encountered in the case of surface

heterogeneity [36] or a porosity of the interface between the metal matrix and the solution [37].

The following equation summarized the impedance of the constant phase elements (*CPE*):

$$Z_{CPE}(\omega) = Q^{-1}(j\omega)^{-n} \quad (5)$$

Q which is a constant with dimensions of $\Omega.cm^{-2}.s^{n}$ and n is the *CPE* exponent with $-1<n<1$. Z_{CPE} can represent an inductance (n=-1), a Warburg impedance (n=0.5), a capacitance (n=1), or a resistance (n=0).

The equivalent electrical circuit that gave the best fit with the experimental curves is shown in Figure 9.

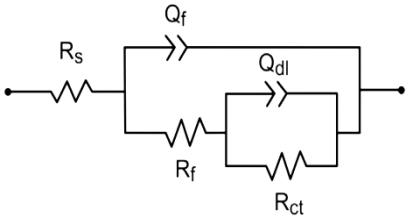

Fig. 9. The equivalent circuit model used to fit the experimental impedance data brasses in sample so l (sol_{mod}) at 14% moisture after 21 days of immersion

Table 5. Electrochemical impedance parameters relative to two series of brass (α -brass and (α + β) brass) after 21 days of immersion in sample soil (sol_{mod})

Brass grad	***Rs*** ***(Ω.cm²)***	***Q_{ct}*** ***(µF/cm²)***	***α_{ct}***	***R_{ct}*** ***(KΩ.cm²)***	***Q_{dif}*** ***(µF/cm²)***	***α_{dif}***	***R_{dif}*** ***(KΩ.cm²)***	***R_p*** ***(KΩ.cm²)***
EC1	137	548	0.66	0.586	46	0.85	10.6	11
EC2	67	349	0.65	1.4	150	0.62	3.7	5
EC4	48	347	0.62	2.8	66	0.97	6.1	8,8
EC6	119	446	0.73	1.7	201	0.50	11.4	13
EC3	131	557	0.65	0.8	223	0.63	8.1	8,7
EC5	151	246	0.64	3.5	199	0.53	6.3	9,6
EC7	54	35	0.64	0.9	199	0.60	5.5	6.4

Examination of Table 5 shows that the man 2 and man 1 samples are respectively the most resistant among the α+β brasses and α -brasses. The classification of these brasses according to their Rp values is presented as follows:

-for α-brasses:

EC1> EC3> EC7.

-for α+β brasses:

EC6> EC1> EC4> EC2.

This result has been previously discussed by the stationary method (polarization curve).

4. CONCLUSION

Polarization curves was associated with EIS techniques to examine the corrosion behavior of two series of brass alloys (brass devices) in a very aggressive environment containing the nitrate ions .The main conclusions can be cited as follow:

- The comparison of the current density values and polarization resistant Rp of the different brass samples in the presence of 2 g/L of $NaNO_3$ reveals that the NO_3^- ions are very aggressive for brass, so the dezincification process has been accelerated. This effect is pronounced in the case of the brass with a single phase α
- The decrease in the corrosion resistance of brass in the presence of nitrate ions is generally due to the local acidification mechanism.
- The existence of Arsenic in α-brass composition improves significantly its resistance to corrosion.
- The existence of Fe and Mn in the brass decreases the corrosion resistance of this alloy.
- All measurements showed that the corrosion resistance of the materials studied can be classified in the following order:

- α-brasses: EC1> EC3> EC7.
- (α +β)-brasses: EC6> EC1> EC4> EC2.

- According to the obtained results in this study, the most resistant is the EC6 alloy

Acknowledgement

Authors are gratefully acknowledges National office of water and electricity (ONEE), Rabat, Morocco for the financial assistance and facilitation of our study.

REFERENCES

[1] D. Chebabe, A. Dermaj, Z. E. A. A. Chikh, H. Ramli, M. Doubi, N. Hajjaji, and A. Srhiri, Anal. Bioanal. Electrochem. 3 (2011) 279.

[2] B. Assouli, A. Srhiri, and H. Idrissi, NDT E Int. 36 (2003) 117.

[3] Y. Jagodzinski, P. Aaltonen, S. Smuk, O. Tarasenko, and H. Hänninen, J. Alloy Compd. 310 (2000) 256.

[4] R. Heidersbach, Corrosion 24 (1968) 38.
[5] R. M. Horton, Corrosion 26 (1970) 160.
[6] A. M. Beccaria, G. Poggi, and G. Capannelli, Corrosion Prev. Contr. 36 (1989) 169.
[7] S. Sohn, and T. Kang, J. Alloy Compd. 335 (2002) 281.
[8] J. Y. Zou, D. H. Wang, and W. C. Qiu, Electrochim. Acta 42 (1997) 1733.
[9] X. Luo, and J. Yu, Corros. Sci. 38 (1996) 767.
[10] C. Fiaud, S. Bensarsa, I. Demesy, and M. Tzinmann, Br. Corros. J. 22 (1987) 109.
[11] K. Tronner, A. G. Nord, and G. Ch. Borg, Water Air Soil Pollut 85 (1995) 2725.
[12] S. A. Fernandez, and M. G. Alvarez, Corros. Sci. 53 (2011) 82.
[13] T. K. G. Namboodhiri, R. S. Chaudhary, B. Prakash, and M. K. Agrawal, Corros. Sci. 22 (1982) 1037.
[14] L. Burzynska, Corros. Sci. 43 (2001) 1053.
[15] T. J. Kagetsu, and W. F. Graydon, J. Electrochem. Soc. 110 (1963) 709.
[16] M. G. Alvarez, P. Lapitz, S. A. Fernandez, and J. R. Galvele, Corros. Sci. 47 (2005) 1643.
[17] M. Galai, J. Ouassir, M. Ebn Touhami, H. Nassali, H.Benqlilou, T. Belhaj, K. Berrami K, I. Mansouri, and B. Oauki , Journal of Bio-and Tribo-Corrosion. 3 (2017) 30.
[18] M. Barbalat, L. Lanarde, D. Caron, M. Meyerb, J. Vittonato, F. Castillon, S. Fontaine, and P. Refait, Corros. Sc. 55 (2012) 246.
[19] A. Bouckamp, Users Manual Equivalent Circuit Ver. 4 (1993) 51.
[20] C. Deslouis, B. Trobolet, G. Mongoli, and M. M. Musiani, J. Appl. Electrochem. 18 (1988) 374.
[21] M. Clément Berne, étude de la sensibilité a la corrosion sous contrainte de laitons biphasés - conception d'un test accélère d'évaluation de la sensibilité a la corrosion sous contrainte de composants de robinetterie gaz, Thesis (2015).
[22] M. M. Sadawy, and M. Ghanem, Technology 12 (2016) 316.
[23] S. A. Fernandez, and M. G. Alvarez, Corros. Sci. 53 (2011) 82.
[24] J. R. Galvele, J. Electrochem. Soc. 123 (1976) 464.
[25] F. W. Fink, Trans. Electrochem. Soc. 75 (1939) 441.
[26] H. O. Curkovic, E. Stupnisek-Lisac, and H. Takenouti. Corros. Sci. 52 (2010) 398
[27] C. Chiavari, A. Colledan, A. Frignani, and G. Brunoro, Mater. Chem. Phys. 95 (2006) 252.
[28] G. D. Bengough, and R. May, J. Instrum. Met. 32 (1924) 81.
[29] R. W. Sullivan, INCRA Project 178 (1971) 47.
[30] J. H. Hollomon, and M. Wulff - Trans. Aimme (1942)
[31] H. Mazille, F. Dabosi, G. Beranger, and B. Baroux, Corrosion localisee. Paris: Editions de Physique (1994) 380.
[32] D. D. Macdonald, Corrosion 46 (1990) 22.

[33] D. D. Macdonald, and M. urquidi-Macdonald, J. Electrochem. Soc. 132 (1985) 231.
[34] M. urquidi-Macdonald, S. Real, and D. D. Macdonald, J. Electrochem. Soc. 133 (1986) 2018.
[35] K. M. Ismail, and W. A. Badawy. J. Appl. Electrochem. 30 (2000) 1303.
[36] W. A. Badawy, F. M. Al Kharafi, Corrosion 55 (1999) 268.
[37] J. B. Jorcin, Spectroscopie d'impédance électrochimique locale: caractérisation de la de lamination des peintures et de la corrosion des alliages Al-Cu, Thesis, INPT, France. (2007).